

lncRNA *FDNCR* promotes apoptosis of granulosa cells by targeting the miR-543-3p/*DCN*/TGF- β signaling pathway in Hu sheep

Xiaolei Yao,^{1,2} XiaoXiao Gao,^{1,2} Yongjin Bao,^{1,2} M.A. El-Samahy,^{1,2} Jinyu Yang,³ Zhibo Wang,^{1,2} Xiaodan Li,^{1,2} Guomin Zhang,^{1,2} Yanli Zhang,^{1,2} Wujun Liu,⁴ and Feng Wang^{1,2}

¹Jiangsu Livestock Embryo Engineering Laboratory, Nanjing Agricultural University, Nanjing 210095, China; ²Hu Sheep Academy, Nanjing Agricultural University, Nanjing 210095, China; ³Biomarker Technologies Corporation, Beijing 101300, China; ⁴College of Animal Science, Xinjiang Agricultural University, Urumqi 830052, China

Long non-coding RNAs (lncRNAs) regulate the development of follicles and reproductive diseases, but the mechanisms by which lncRNAs regulate ovarian functions and fertility remain elusive. We profiled the expression of lncRNAs in ovarian tissues of Hu sheep with different prolificacy and identified 21,327 lncRNAs. Many of the lncRNAs were differentially expressed in different groups. We further characterized an lncRNA that was predominantly expressed in the ovaries of the low prolificacy *Fec*^{B+} (LPB+) group and mainly present in granulosa cells (GCs), and the expression of this lncRNA decreased during follicular development, which we named follicular development-associated lncRNA (*FDNCR*). Next, we found that *FDNCR* directly binds miR-543-3p, and decorin (*DCN*) was identified as a target of miR-543-3p. *FDNCR* overexpression promoted GC apoptosis through increased expression of *DCN*, which could be attenuated by miR-543-3p. Furthermore, miR-543-3p increased and *FDNCR* reduced the expression of transforming growth factor- β (TGF- β) pathway-related genes, including *TGF- β 1* and inhibin beta A (*INHBA*), which were upregulated upon *DCN* silencing. Our results demonstrated that *FDNCR* sponges miR-543-3p in GCs and prevents miR-543-3p from binding to the *DCN* 3' UTR, resulting in *DCN* transactivation and TGF- β pathway inhibition and promotion of GC apoptosis in Hu sheep. These findings provide insights into the mechanisms underlying prolificacy in sheep.

INTRODUCTION

Low reproductive efficiency (i.e., litter size) limits the development of the sheep industry. Most sheep species exhibit seasonal estrus and produce one lamb per pregnancy. Thus, good breed selection is important for crossbreeding. Hu sheep are an excellent local breed in China and are famous for their precocious puberty, year-round estrus, and high fecundity (average litter size 2.06).¹ Granulosa cells (GCs) play an essential role in the recruitment, selection, ovulation, and atresia of follicles.² Therefore, elucidation of GC function is important for understanding follicular development, increasing the ovulation rate, and female fertility. This will provide useful information for the breeding and trait selection of Hu sheep.

FecB (*BMPRI3* mutation) is a fundamental fecundity gene in Hu sheep.² Sheep with the homozygous mutation (*Fec*^{BB} [BB]) exhibit higher ovulation rates than do heterozygous (*Fec*^{B+} [B+]) or wild-type (++) sheep.^{3–5} However, under similar conditions, some Hu sheep carrying the BB mutation gave birth to single lambs, although the underlying molecular mechanisms remain unknown.

Long non-coding RNAs (lncRNAs) with length >200 nt regulate genes at the transcriptional and post-transcription levels. At the post-transcriptional level, lncRNA can serve as efficient microRNA (miRNA) sponges—termed competing endogenous RNAs (ceRNAs)—that interact with miRNA to regulate gene expression.⁶ Recently, numerous lncRNAs have been identified in humans and other organisms that play diverse roles in regulating various phenomenon, such as cell proliferation and apoptosis,^{7,8} cell development,⁹ cell differentiation,¹⁰ and development of certain diseases.^{11,12} Specifically, lncRNAs are involved in regulating spermatogenesis,^{13,14} steroidogenesis,¹⁵ embryo implantation¹⁶ and development,¹⁷ follicular development,¹⁸ oocyte maturation,¹⁹ GC apoptosis and proliferation,^{20,21} and reproductive diseases,^{22,23} suggesting their importance in reproduction.²⁴ However, only a few lncRNAs have been identified in domestic animals. Although lncRNA expression profiles in the ovary, uterus, and pituitary glands of sheep^{25–31} (Small Tail Han sheep, Dorset sheep, or Hu sheep), and goats³² (Anhui white goats) with different prolificacy indicate their importance in determining female fecundity, the mechanisms underlying the influence of lncRNA with respect to determining fecundity in Hu sheep remain elusive.

GC apoptosis can result in follicular atresia, a key process in follicle selection and development.^{33–35} Only 1% of the follicles eventually mature and ovulate, and >99% undergo atresia and degeneration in mammals.³⁶ Although GC apoptosis is regulated by lncRNAs such

Received 21 October 2020; accepted 24 February 2021;
<https://doi.org/10.1016/j.omtn.2021.02.030>

Correspondence: Feng Wang, Jiangsu Livestock Embryo Engineering Laboratory and Hu Sheep Academy, Nanjing Agricultural University, Nanjing 210095, China.
E-mail: caet@njau.edu.cn



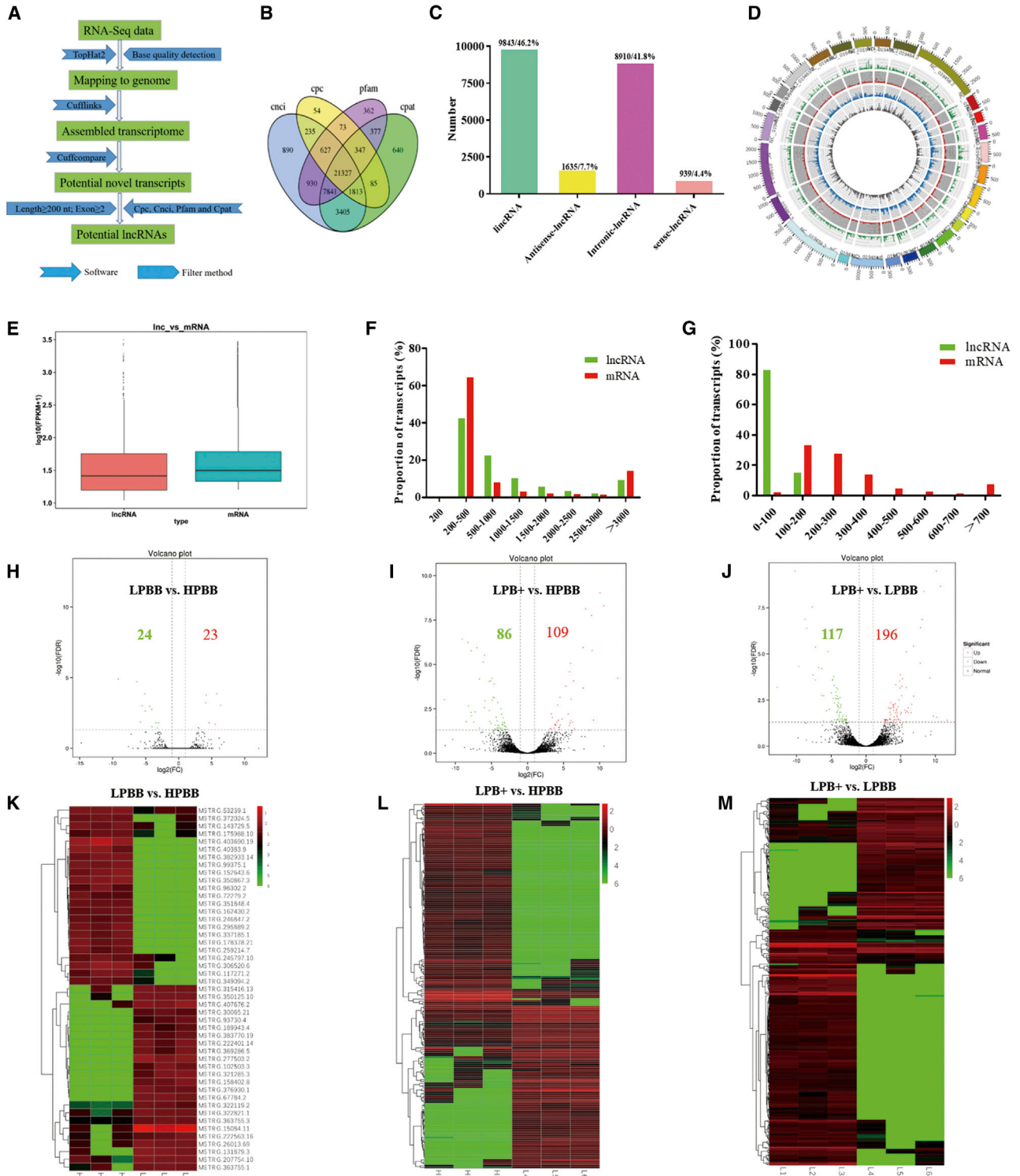


Figure 1. Profile of lncRNA expression in the ovaries of Hu sheep and identification of DE lncRNAs

(A) Workflow for the preparation and analysis of lncRNA libraries. (B) Identification of lncRNAs in the ovarian tissue of Hu sheep. (C) Classification of lncRNAs. (D) Circos plot showing the distribution of lncRNAs in different chromosomes. The outermost ring represents different chromosomes. From the outside toward the inside: sense-lincRNA

(legend continued on next page)

as *PVT1* and *NORFA*,^{22,37} the number of lncRNAs reported to be involved in GC apoptosis and follicular development remains limited.

In this study, we hypothesized that the differences in fecundity and *FecB* genotype could be correlated with different lncRNA expression profiles in the ovarian cells of Hu sheep, providing a target for treating ovulation failure. Hence, we investigated the differentially expressed (DE) lncRNAs in the ovaries of Hu sheep with different prolificacy (high prolificacy [HP], litter size = 3; low prolificacy [LP], litter size = 1) and *FecB* genotypes (BB and B+) using RNA sequencing (RNA-seq). We further characterized that a follicular development-associated lncRNA (*FDNCR*) acts as a ceRNA for miR-543-3p to augment decorin (*DCN*) expression and inhibit the transforming growth factor- β (TGF- β) signaling pathway, thereby promoting GC apoptosis in Hu sheep. The findings of our study would aid in extensively improving sheep breeding in China and would provide insights into the regulatory mechanisms responsible for determining the fecundity of Hu sheep. Additionally, this study also may provide a basis for identifying new therapeutic strategies for reproductive diseases, such as polycystic ovarian syndrome (PCOS), which leads to ovulation failure.

RESULTS

Identification of DE lncRNA in the ovaries of Hu sheep

To identify putative transcripts in sheep ovaries, nine ovarian samples were obtained from different groups (HPBB, LPBB and LPB+). We acquired 59–83, 58–71, and 54–66 million unique mapped clean reads in LPB+, LPBB, and HPBB libraries, respectively (Table S1). Many lncRNAs were identified in Hu sheep ovaries according to the steps of the workflow shown in Figure 1A. In total, 21,327 lncRNAs were identified in Hu sheep ovaries (Figure 1B), including 9,843 long intergenic non-coding RNA (lincRNAs), 8,910 intronic lncRNAs, 1,635 anti-sense lncRNAs, and 939 sense lncRNAs (Figure 1C). Despite the non-uniform distribution of the lncRNA-coding sequences among the chromosomes, the number of reads mapped to the chromosome increased with increasing chromosome length (Figure 1D). The lncRNA expression level was lower than that of mRNA in Hu sheep ovaries (Figure 1E). lncRNA distribution transcripts were mainly located from 200 to 1,000 bp (Figure 1F). The lengths of the open reading frame coding for the lncRNAs and mRNA transcripts were in the range 0–100 bp and 100–300 bp, respectively (Figure 1G).

There were 47 (23 upregulated and 24 downregulated), 195 (109 upregulated and 86 downregulated), and 313 (196 upregulated and 117 downregulated) DE lncRNAs identified in the LPBB versus HPBB (Figure 1H; Table S2), LPB+ versus HPBB (Figure 1I; Table S3), and LPB+ versus LPBB groups (Figure 1J; Table S4), respectively. Hierarchical clustering of the DE lncRNAs (Figures 1K–1M) revealed the expression patterns of the individuals for the same three compar-

isons. Additionally, we found non-uniform distribution of DE lncRNAs across the chromosomes (Figure S1).

To further evaluate RNA-seq reliability, seven DE lncRNA transcripts were randomly selected for quantitative reverse transcriptase PCR (qRT-PCR). The results obtained were consistent with those of RNA-seq, indicating the reliability of the RNA-seq data (Figure S2).

Functional enrichment and construction of lncRNA-mRNA interaction network

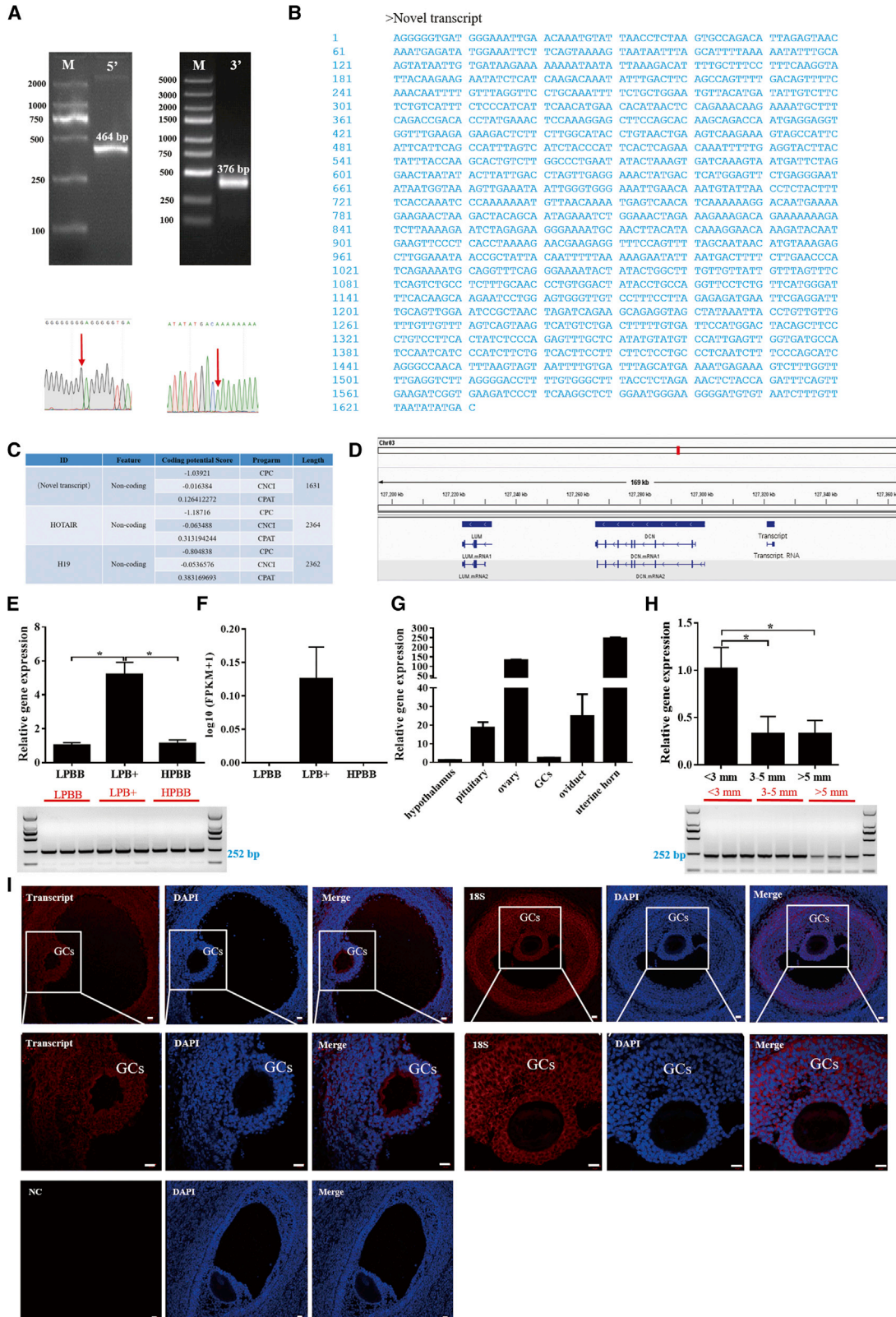
The roles of DE lncRNAs could be revealed by enrichment analyses of their target genes through Gene Ontology (GO) and the Kyoto Encyclopedia of Genes and Genomes (KEGG). The female reproduction-associated 4, 26, and 44 DE lncRNAs were screened in the LPBB versus HPBB (Table S5), LPB+ versus HPBB (Table S6), and LPB+ versus LPBB (Table S7) groups, respectively. Notably, DE lncRNA targets were most commonly enriched in reproductive signaling pathways, including TGF- β , prolactin, and insulin in the LPB+ versus HPBB and LPB+ versus LPBB groups. Moreover, certain DE lncRNAs (1, 2, and 2, respectively) were specifically expressed in the HPBB (Table S8), LPBB (Table S9) and LPB+ (Table S10) groups, indicating the potential role of these DE lncRNAs in Hu sheep prolificacy. Notably, MSTRG.98424.7 was predominantly expressed in the ovaries of the LPB+ group and had two nearly coding genes (*DCN* and *LUM*), wherein *DCN* is an intermediary of the TGF- β signaling pathway. Furthermore, a co-expression network was constructed for female reproduction-associated DE lncRNAs (Figure S3), which provided valuable information regarding the potential function of the analyzed lncRNAs with respect to regulating the expression of their target genes.

Identification and characterization of candidate lncRNAs

The 1,631-nt full-length sequence of the MSTRG.98424.7 transcript was generated using 5' and 3' rapid amplification of cloned cDNA ends (RACE; Figures 2A and 2B). The non-coding nature of this transcript was confirmed by coding-potential analysis, similar to other well-characterized lncRNAs, HOTAIR and H19 (Figure 2C; Figure S4). Furthermore, the transcript was located upstream of *DCN* and *LUM* on sheep chromosome 3 and consisted of two exons (Figure 2D). Moreover, compared with *FDNCR*, a region exhibiting high homology (65.54%) with LOC105607925 (known lncRNA in *Ovis aries* genome) (Figure S5A), annotated upstream of *DCN* and *LUM*, was observed at sheep chromosome 3 and consisted of five exons (Figure S5B).

Compared with either LPBB or HPBB group, both the expression level (Figure 2E) and RNA-seq (Figure 2F) of this transcript were significantly higher in the LPB+ group, indicating the high accuracy of the RNA-seq data. Notably, the transcript was highly expressed

(green), lincRNA (red), intronic-lncRNA (blue), and antisense-lncRNA (gray). (E) Boxplots showing the expression levels of lncRNAs and mRNAs. FPKM, fragments per kilobase of transcript per million mapped reads. (F) Length of lncRNAs and mRNAs. (G) Lengths of open readings frames of lncRNAs and mRNAs. (H–J) Volcano plot of DE lncRNAs in each group. FDR, false discovery rate; FC, fold change. Red indicates upregulated and green indicates downregulated. (K–M) Hierarchical clustering of DE lncRNAs in each group.



(legend on next page)

in the uterine horn and ovary, from the LPBB group of Hu sheep, with low expression in the hypothalamus (Figure 2G). Moreover, the transcript expression was reduced during follicular development, as determined by the follicle diameter (Figure 2H). Fluorescence *in situ* hybridization (FISH) indicated that the transcript was mainly expressed in the GCs and theca cells of the LPBB group (Figure 2I). Hence, the candidate transcript was termed *FDNCR* based on these characteristics.

***FDNCR* is involved in GC apoptosis and proliferation**

To determine the function of *FDNCR* in follicular development, we overexpressed and knocked down *FDNCR* in GCs using small interfering RNA (siRNA) and found that the transcript levels of *FDNCR* were significantly increased and decreased, respectively (Figures 3A and 3B). The 5-ethynyl-2'-deoxyuridine (EdU) assay indicated that overexpression or knockdown of *FDNCR* significantly inhibited and promoted cell proliferation, respectively (Figures 3C and 3D), which was consistent with the results obtained using the Cell Counting Kit-8 (CCK8) assay (Figure 3E). *FDNCR* overexpression and knockdown promoted (14.08% ± 0.51% versus 20.31% ± 0.35%) and inhibited (36.27% ± 2.81% versus 25.13% ± 3.36%) GC apoptosis, respectively (Figure 3F). Moreover, *FDNCR* overexpression significantly downregulated *CDK1* and *CyclinD1* and upregulated *BAX* and the *BAX/Bcl-2* ratio although not *CyclinB1* and *Bcl-2* mRNA expression; *FDNCR* knockdown dramatically upregulated *CDK1*, *CyclinB1*, and *Bcl-2*, although not *CyclinD1* mRNA expression, and it downregulated *BAX* mRNA expression and the *BAX/Bcl-2* ratio (Figure 3G). Similarly, PCNA and *Bcl-2* protein expression levels were significantly downregulated or upregulated upon *FDNCR* overexpression and knockdown, respectively (Figure 3H). Furthermore, *BAX* protein abundance and the *BAX/Bcl-2* ratio were significantly decreased upon *FDNCR* knockdown, whereas no change was observed upon *FDNCR* overexpression (Figure 3H). Overall, our data indicated that *FDNCR* plays vital roles in follicular development by promoting GC apoptosis.

***FDNCR* acts as a ceRNA for miR-543-3p**

Because subcellular localization (nuclear or cytoplasmic) of lncRNAs may influence its functions, subcellular fractionation analyses were performed, which revealed that >65% of *FDNCR* was localized to the cytoplasm of GCs (Figure 4A); this was further confirmed using FISH (Figure 4B). Furthermore, the *FDNCR*-binding miRNAs miR-543-3p, miR-541-5p, miR-377-5p, and miR-125b were predicted as candidates using RNAhybrid and miRanda software (Figure 4C). A ceRNA (*FDNCR*-miRNA-mRNA) network with four miRNAs and 16 mRNAs was constructed in Hu sheep and belongs to the TGF-β signaling pathway (Figure 4D).

The highest and lowest expression levels of miR-543-3p were in the HPBB group with >5-mm healthy follicles and the LPB+ group with <3-mm healthy follicles, respectively; both groups were negatively correlated with *FDNCR* expression (Figures 4E and 4F). Although miR-541-5p expression in the ovaries from LPBB was significantly higher than that in the LPB+ and HPBB groups, a correlation with *FDNCR* expression was not apparent (Figure S6A). Moreover, miR-541-5p expression increased with increasing follicle diameter and was negatively correlated with *FDNCR* expression (Figure S6B). Thus, miR-543-3p and miR-541-5p may be involved in follicular development.

To further investigate the miRNA directly binding to *FDNCR*, qRT-PCR was performed. miR-543-3p was significantly downregulated and upregulated upon *FDNCR* overexpression and silencing in GCs, respectively (Figures 4G and 4H). Moreover, miR-543-3p levels increased and decreased after treatment with miR-543-3p mimics and inhibitors, respectively (Figures 4I and 4J). Dual-luciferase reporter constructs containing the miRNA response element (MRE; wild-type [WT]) and mutant (mut) plasmid were co-transfected with miR-543-3p mimics into GCs (Figure 4K). Luciferase activity of the *FDNCR*-MT construct was dramatically decreased, although that for the *FDNCR*-mut construct did not change (Figure 4L). Meanwhile, miR-543-3p overexpression or knockdown had no effect on *FDNCR* expression in GCs from Hu sheep (Figures 4M and 4N). Moreover, the RNA-binding protein immunoprecipitation (RIP) assay was performed using AGO2 antibody, followed by qRT-PCR, confirming the interaction between *FDNCR* and miR-543-3p (Figure 4O). These data indicated that *FDNCR* may act as a ceRNA to sponge miR-543-3p.

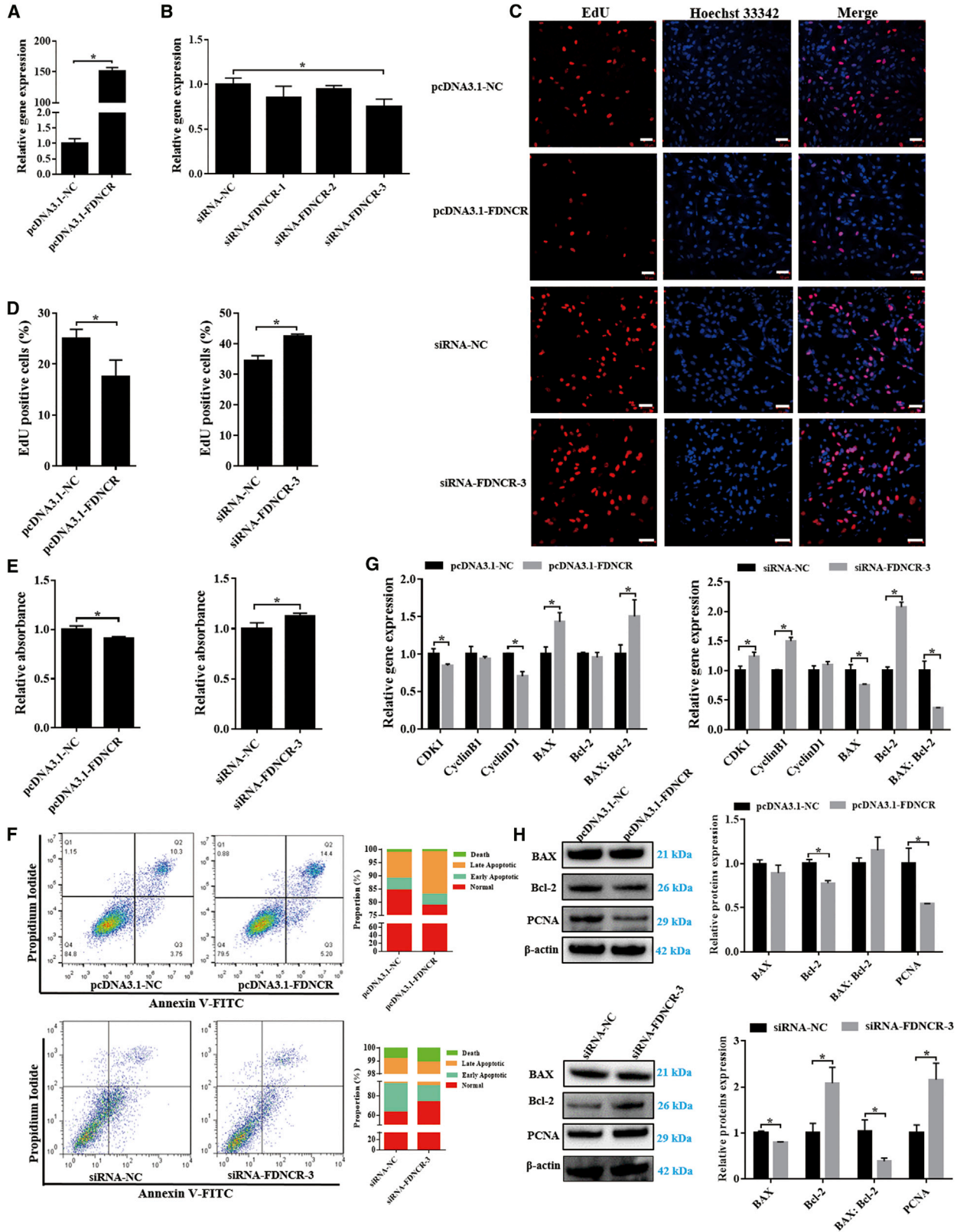
Next, we isolated and characterized the gene encoding miR-543-3p, which is 123 bp in length and conserved among sheep and other mammals such as goats and cows (Figure S7A). The mature sequences of miR-543-3p and the seed region of miR-543-3p are also highly conserved in other species (Figure S7B). Therefore, these results clearly demonstrated that miR-543-3p is evolutionarily conserved in mammals.

***FDNCR* inhibits the proliferation of GCs by sponging miR-543-3p in Hu sheep**

We further explored the critical functions of miR-543-3p in GCs, and the results showed that miR-543-3p mimics reduced apoptosis (10.91% ± 0.94% versus 7.76% ± 0.08%), *BAX* mRNA expression, and the *BAX/Bcl-2* ratio, whereas it elevated the mRNA and/or protein expression of *Bcl-2* and PCNA (Figures 5A–5C). However,

Figure 2. Identification and characterization of a candidate transcript in Hu sheep

(A) Representative images from RACE (5' RACE and 3' RACE) and Sanger DNA sequencing. (B) The full-length RNA sequence of this transcript. (C) The coding potential of this transcript and other RNAs was predicted using three computational approaches (CPC, coding potential calculator; CNCI, coding-non-coding index; CPAT, coding potential assessment tool). (D) Schematic view of the chromosomal location of this transcript. (E and F) Expression levels of this transcript in each group using qRT-PCR (E) and RNA-seq (F). (G and H) Expression level of this transcript in different tissues of the LPBB group (G) and healthy follicles of various sizes (H) from Hu sheep. (I) Localization of the transcript in the ovaries was detected by FISH. GC, granulosa cell. Scale bars, 20 μm. RNA-seq data are presented as the log₁₀(FPKM+1) of each transcript. Values represent means ± SEM for three individuals. *p < 0.05.



(legend on next page)

miR-543-3p overexpression had no effect on BAX protein levels or the BAX/Bcl-2 protein ratio (Figure 5C). In contrast, miR-543-3p inhibitor treatment increased apoptosis ($8.43\% \pm 0.60\%$ versus $9.95\% \pm 0.39\%$), BAX mRNA and protein expression, and the BAX/Bcl-2 ratio, and it reduced Bcl-2 mRNA and protein expression; however, miR-543-3p knockdown exerted no effect on PCNA protein levels (Figures 5A–5C). EdU and CCK8 assays showed that miR-543-3p mimics promoted GC proliferation, although cell growth was retarded upon miR-543-3p inhibitor treatment (Figures 5D–5F). miR-543-3p mimics significantly upregulated *CDK1*, *CyclinD1*, and *CyclinB1* mRNA expression, whereas miR-543-3p inhibitor significantly downregulated *CDK1* and *CyclinB1* expression (Figure 5G). These data indicated that miR-543-3p functioned as an anti-apoptotic epigenetic regulator in GCs.

Mediation of *FDNCR* functioning by miR-543-3p was further investigated. The results showed that overexpression of miR-543-3p rescued apoptosis ($27.45\% \pm 2.60\%$ versus $21.27\% \pm 1.65\%$) caused by *FDNCR* overexpression, *FDNCR*-induced BAX mRNA expression, and the BAX/Bcl-2 ratio, and it reduced Bcl-2 mRNA expression; conversely, inhibition of miR-543-3p prevented *FDNCR*-specific siRNA reduced apoptosis ($12.19\% \pm 0.57\%$ versus $19.17\% \pm 1.10\%$), and *FDNCR*-siRNA reduced BAX mRNA expression and the BAX/Bcl-2 ratio (Figures 5H and 5I). Thus, *FDNCR* promoted apoptosis by sponging miR-543-3p in GCs from Hu sheep.

miR-543-3p regulates GC proliferation by targeting *DCN*

Based on the above ceRNA (*FDNCR*-miR-543-3p-mRNA) network, several genes (e.g., *DCN* and *ACVR2A*) were predicted to be miR-543-3p target genes. Software analysis showed that the miR-543-3p seed sequence was completely paired with the *DCN* 3' UTR (Figure 6A). Luciferase reporter plasmids containing the *DCN*-MT MRE motif or the mutated versions were constructed (Figure 6B) and co-transfected with miR-543-3p mimics into GCs. miR-543-3p significantly reduced luciferase activity of the reporter containing the MRE-MT motif, with no change in reporter activity observed with the mutant MRE motif (Figure 6C), indicating that *DCN* is a direct target of miR-543-3p. Furthermore, miR-543-3p mimics and inhibitor markedly downregulated and upregulated *DCN* mRNA and protein expression levels in GCs, respectively (Figures 6D and 6E). Collectively, these results implied that *DCN* is a functional target of miR-543-3p in GCs of Hu sheep. *DCN* was predominantly localized in GCs in all follicle types and predominantly localized in the cytoplasm of cultured GCs (Figures S8A and SB). Additionally, the highest expression of *DCN* was noted in the uterine horn and ovary (Figure S8C), and expression increased with follicle diameter, although no significant difference was observed (Figure S8D), suggesting that *DCN* is important in follicular development.

We investigated the potential functions of *DCN* in GCs from Hu sheep. The synthesized expression vector pcDNA3.1-*DCN* and *DCN*-specific siRNA (siRNA-*DCN*-1) increased and decreased *DCN* mRNA and protein levels, respectively (Figures 7A–7D). Notably, *DCN* overexpression by pcDNA3.1-*DCN* transfection and *DCN* knockdown by siRNA-*DCN*-1 inhibited and promoted GC proliferation, respectively (Figures 7E–7G). *DCN* overexpression and knockdown significantly promoted ($17.13\% \pm 3.32\%$ versus $31.20\% \pm 2.25\%$) and inhibited ($41.38\% \pm 3.28\%$ versus $19.91\% \pm 3.33\%$) GC apoptosis, respectively (Figure 7H). Moreover, *DCN* overexpression significantly downregulated *CDK1* and *CyclinB1* mRNA expression, as well as the BAX/Bcl-2 ratio; however, *DCN* overexpression had no effect on *CyclinD1*, BAX, and Bcl-2 mRNA levels (Figure 7I). Furthermore, *DCN* knockdown significantly upregulated *CDK1*, *CyclinD1* and Bcl-2 mRNA levels and downregulated BAX mRNA expression and the BAX/Bcl-2 ratio; however, *CyclinB1* mRNA expression was not significantly affected (Figure 7I). Furthermore, *DCN* overexpression significantly upregulated BAX protein expression and the BAX/Bcl-2 ratio, and it downregulated PCNA protein levels, whereas the opposite trend was observed in the *DCN* knockdown group (Figure 7J). Overall, these data suggest that *DCN* is a pro-apoptotic regulator in GCs from Hu sheep.

We further investigated the regulation of GC apoptosis by *DCN*-mediated miR-543-3p. miR-543-3p mimic or inhibitor and pcDNA3.1-*DCN* or siRNA-*DCN*-1 were co-transfected into GCs. Overexpression of *DCN* reduced the anti-apoptotic effect of miR-543-3p mimics ($11.37\% \pm 0.22\%$ versus $17.43\% \pm 2.69\%$), whereas apoptosis ($11.92\% \pm 0.79\%$ versus $10.36\% \pm 0.75\%$) induced by miR-543-3p inhibitor was recovered when *DCN* was knocked down (Figure 7K). Overall, these data strongly suggest that miR-543-3p regulates GC apoptosis by targeting *DCN*.

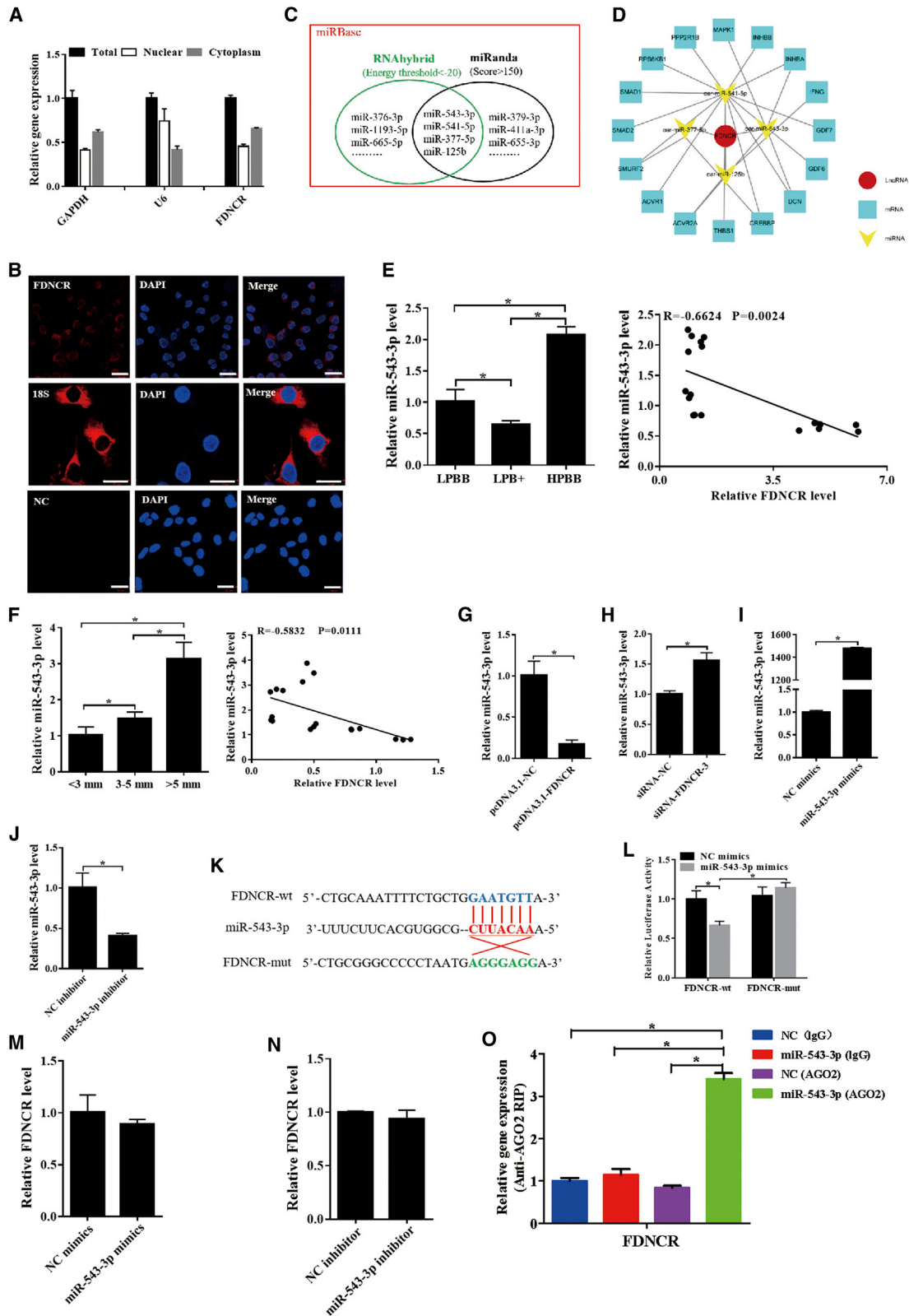
FDNCR regulates the TGF- β pathway via miR-543-3p-*DCN* axis

We investigated the mechanism through which *FDNCR* acted as an upstream regulator of miR-543-3p to affect *DCN* expression. Notably, ovarian *FDNCR* expression in Hu sheep with different prolificacy was positively correlated with *DCN* mRNA levels (Figure 8A). *DCN* mRNA levels were significantly upregulated and downregulated in GCs after transfection with pcDNA3.1-*FDNCR* and siRNA-*FDNCR*-3, respectively (Figure 8B), which indicates that *FDNCR* is a regulator of *DCN*. Moreover, miR-543-3p mimics inhibited *FDNCR*-induced *DCN* mRNA expression, and miR-543-3p inhibitor rescued siRNA-*FDNCR*-3-reduced *DCN* expression (Figure 8C). These data indicated that miR-543-3p mediated *FDNCR*-induced *DCN* expression in GCs of Hu sheep.

DCN inhibits TGF- β by binding to its receptors, which leads to interference with the Smad and non-Smad pathways downstream of the

Figure 3. *FDNCR* promotes Hu sheep GC apoptosis

(A and B) mRNA expression of *FDNCR* in GCs in each group. (C–F) GC proliferation and apoptosis were detected using EdU (C and D), CCK8 (E), and flow cytometry (F). Scale bars, 50 μ m. (G and H) mRNA (G) and protein (H) expression of cell cycle- and/or apoptosis-related genes in GCs in each group. Values represent means \pm SEM for three individuals. * $p < 0.05$.



(legend on next page)

TGF- β receptors.^{38–40} Therefore, RNA-seq was performed to elucidate genes downstream of *DCN* after transfection with siRNA-*DCN-1* in GCs, and that of the TGF- β signaling pathway was noted. RNA-seq data quality was verified by correlation coefficient trends; hence, further analyses were performed (Figure 8D). 15 downregulated and 60 upregulated DE genes were identified (Figure 8E; Table S11), and hierarchical clustering thereof revealed expression profiles involving the siRNA-negative control (NC) and siRNA-*DCN* groups (Figure 8F). TGF- β signaling pathway-related genes, including *TGF- β 1* and inhibin beta A (*INHBA*), were upregulated upon *DCN* silencing and exhibited similar expression patterns (Figure 8G).

Furthermore, we investigated the interaction between the *FDNCR*-miR-543-3p axis and *TGF- β 1* and *INHBA*. *FDNCR* overexpression downregulated *TGF- β 1* and *INHBA* mRNA or protein expression, and the mRNA or protein levels of *INHBA*, although not *TGF- β 1*, were significantly increased after *FDNCR* knockdown (Figure 8H). However, miR-543-3p mimics increased *TGF- β 1* and *INHBA* mRNA or protein levels, whereas expression of *INHBA*, although not *TGF- β 1*, mRNA or protein was downregulated upon miR-543-3p knockdown (Figure 8I). Moreover, miR-543-3p increased *FDNCR*-reduced *TGF- β 1* and *INHBA* mRNA or protein expression. Conversely, miR-543-3p inhibitor decreased *FDNCR*-induced *INHBA*, although not *TGF- β 1*, mRNA or protein levels (Figure 8J). Collectively, these results indicated that the miR-543-3p-*DCN* axis could have mediated *FDNCR* function in the TGF- β pathway in GCs from Hu sheep (Figure 8K).

DISCUSSION

RNA-seq data revealed that most lncRNAs, which may be byproducts of mRNA, showed low expression levels in ovarian tissue from Hu sheep. However, several abundant DE lncRNAs were identified in Hu sheep with different prolificacy. Moreover, the targets of DE lncRNAs were enriched in certain signaling pathways involved in female reproduction and GC functions, such as the prolactin,⁴¹ insulin,⁴² ovarian steroidogenesis,⁴³ and TGF- β signaling pathways,⁴⁴ suggesting that DE lncRNAs have specific roles in regulating fecundity in Hu sheep. Therefore, consistent with previous reports, lncRNAs might be associated with fecundity in sheep or goats.^{25–29,31,32} Moreover, *FDNCR* was highly expressed in the uterine horn and ovary, and expression levels decreased with increasing follicle diameters, suggesting that *FDNCR* is important for follicular development.

In this study, we demonstrated that *FDNCR* controls follicular development by regulating GC apoptosis and proliferation. Follicular

atresia decreases the number of ovulations and restricts reproductive potential.⁴⁵ *FDNCR* was predominantly expressed in the ovaries of the LPB+ group, indicating that *FDNCR* was involved in fecundity by promoting follicular atresia. *FDNCR*, which is highly expressed in the ovaries of the LPB+ group, may provide insight into the mechanisms through which lncRNA regulates fecundity in sheep. Further studies to investigate other functions of *FDNCR* in regulating GCs (e.g., steroidogenesis), follicular development, or ovulation *in vivo* and reproductive performance such as litter size in Hu sheep are required.

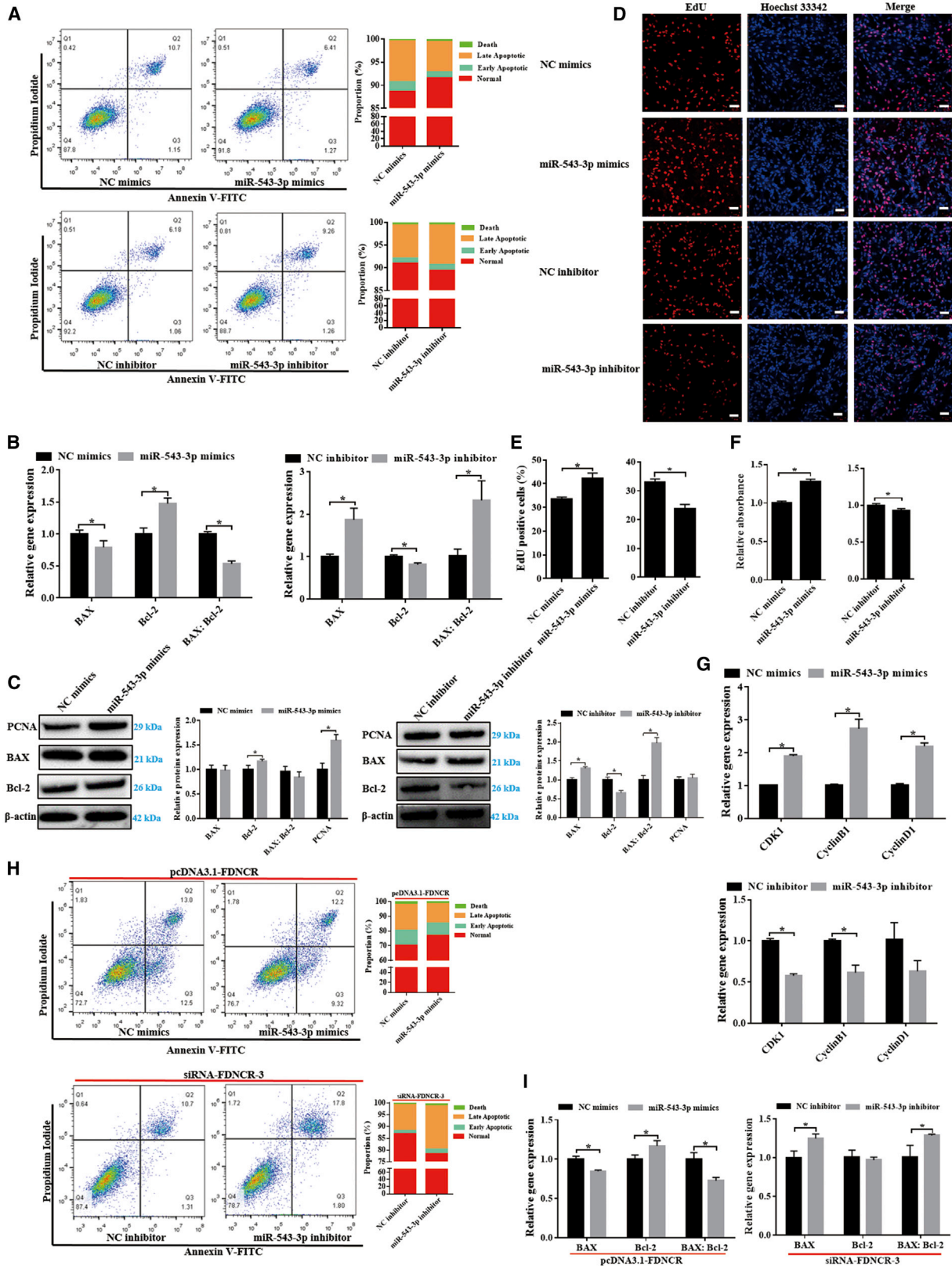
lncRNAs are known to modulate post-transcriptional regulation by acting as miRNA sponges to decrease their target mRNAs.^{46,47} NORFA reportedly regulates porcine GC apoptosis by sponging miR-126.³⁷ lncRNAs *PTVI* and *PCAT6* act as ceRNAs to sponge miR-543 to regulate *SERPINI1* and *ZEB1* expression, respectively.^{48,49} In the present study, we found that *FDNCR* sponged miR-543-3p to negatively regulate miR-543-3p function in GC proliferation and apoptosis. Alternatively, miR-543-3p promoted GC proliferation, which was consistent with previous studies.^{50–52} This effect could be eliminated by *FDNCR* overexpression, suggesting that *FDNCR* regulates GC apoptosis or proliferation by sponging miR-543-3p. These results further demonstrated that *FDNCR* could serve as a regulator of follicular development.

Notably, our results showed that miR-543-3p targeted *DCN*. Several studies have indicated that *DCN* is widely expressed in reproductive tissues, including the ovary and uterus of goats, mice, sheep, and monkeys.^{53–56} Consistently, *DCN* was highly expressed in the ovary, particularly in GCs and the uterine horn from the LPBB group of Hu sheep, suggesting its involvement in the regulation of follicular development. Moreover, miR-543-3p and *DCN* in GCs produced opposing effects, whereby *DCN* promoted GC apoptosis in Hu sheep. Consistently, *DCN* overexpression can induce GC apoptosis or suppress cell proliferation in goat and hamster ovaries.^{53,57} These observations indicate that miR-543-3p regulates GC apoptosis or proliferation by targeting *DCN*. Furthermore, *FDNCR* overexpression increased *DCN* expression, whereas this effect was eliminated by miR-543-3p. This result further demonstrated that binding of *FDNCR* to miR-543-3p regulates GC state and function by targeting *DCN*. Similarly, *LSAMP-AS1* binds to miR-183-5p to suppress prostate cancer progression by upregulating *DCN* gene expression.⁵⁸

DCN can inhibit TGF- β by binding to its receptors, leading to interference with the Smad and non-Smad pathways downstream of TGF- β receptors.^{38–40} In the present study, *TGF- β 1* and *INHBA* genes were

Figure 4. *FDNCR* acts as a ceRNA and sponges miR-543-3p in the GCs of Hu sheep

(A and B) Subcellular localization of *FDNCR* was determined using qRT-PCR (A) and FISH (B). NC, negative control. Scale bars, 20 μ m. (C) RNAhybrid and miRanda predicted that miRNA targets *FDNCR*. (D) Construction of the ceRNA network. (E and F) Expression levels of miR-543-3p in each group. Pearson's correlation was determined between *FDNCR* and miR-543-3p. (G–J) Expression of miR-543-3p in the GCs in each group. (K) Schematic depicting the interactions of miR-543-3p with wild-type *FDNCR* (blue) and mutant *FDNCR* (green). Red nucleotides indicate the seed sequence of miR-543-3p. (L) The regulatory relationship between *FDNCR* and miR-543-3p was assessed using a dual-luciferase reporter gene assay. (M and N) Expression of *FDNCR* in the GCs in each group. (O) Association of *FDNCR* and miR-543-3p with AGO2 was investigated using the RIP assay. *FDNCR* and miR-543-3p expression was quantified by qRT-PCR. Values represent means \pm SEM for three individuals. * $p < 0.05$.



(legend on next page)

upregulated during *DCN* silencing. Increasing evidence has demonstrated that lncRNA or miRNA directly interacts with the TGF- β pathway to regulate the state and function of GCs.^{37,59,60} Notably, this study demonstrated that miR-543-3p restored *TGF- β 1* and *INHBA* expression upon *FDNCR* overexpression. Hence, those results confirmed that the *FDNCR*-miR-543-3p axis interacts with the TGF- β pathway.

In conclusion, numerous lncRNAs with different abundance in Hu sheep ovaries with different prolificacy were annotated. We further identified *FDNCR*, which is predominantly expressed in the ovaries of the LPB+ group and involved in follicular development. Our findings confirm the mechanism whereby *FDNCR* sponges miR-543-3p in GCs and prevents miR-543-3p binding to the *DCN* 3' UTR, which subsequently releases *DCN* and blocks the TGF- β pathway to promote GC apoptosis in Hu sheep. Ovulation is the culmination of female reproductive activity and is essential for successful pregnancy; hence, most female reproductive diseases, such as PCOS, are caused by ovulation defects. Recently, a number of lncRNAs implicated in PCOS, such as lncRNA PVT1 and HOTAIR, have been identified.^{22,23} Therefore, this study identified a candidate lncRNA (*FDNCR*) involved in Hu sheep fecundity, providing insights into the regulatory mechanisms underlying follicular development, which will provide a basis for new therapeutic strategies of reproductive diseases.

MATERIALS AND METHODS

Animals and sample collection

Hu sheep were raised at the Taizhou Sheep Farm (Jiangsu, China) under similar conditions, with free access to food and water and under natural lighting. Twenty non-pregnant healthy ewes (2~3 years age) with identical litter size numbers of three records were randomly selected and divided into HP (each records of litter size=3; n = 4) and LP (each records of litter size=1; n = 16) groups.^{3,61} Finally, nine ewes were selected and divided into HPBB (n = 3), LPBB (n = 3), and LPB+ groups (n = 3). Synchronous estrus was established as described previously.²⁶ The estrus status of the ewes was checked daily. Ewes were slaughtered within 12 h during the estrus stage, and ipsilateral ovary and female reproductive organs (oviduct, uterine horn, hypothalamus, and pituitary) were immediately stored at -80°C. The other ovary was fixed in 4% formaldehyde for 24 h and embedded in paraffin for further analysis. *BMPRIIB* polymorphism genotyping and ovarian morphological characteristic results are shown in Figure S9. All experimental procedures, including animal care, were approved by the Institutional Animal Care and Use Committee of Nanjing Agricultural University (SYXK 2011-0036).

RNA-Seq and bioinformatics analysis

Total RNA was extracted from ovarian tissue of nine ewes, assessed by electrophoresis, and quantified using a NanoDrop 2000 (NanoDrop

Technologies, Wilmington, DE, USA). Library preparation and Illumina sequencing analysis were performed as previously described.²⁹ Unknown transcripts were used to screen putative lncRNAs, as described previously.²⁶ To investigate interactions between lncRNAs and mRNAs, we constructed a complementary pair network comprising mRNA and lncRNA using Cytoscape 3.7.1 (<https://cytoscape.org/>).⁶² The coding potential of *FDNCR* was analyzed by PhyloCSF and open reading frame (ORF) Finder (<https://www.ncbi.nlm.nih.gov/orffinder/>). Venn diagram indicating the intersected genes was generated using a draw Venn diagram online tool (<http://bioinformatics.psb.ugent.be/webtools/Venn/>). Heatmaps were generated by using the R package (heatmap). The raw sequencing dataset supporting the results of this study have been submitted to NCBI Sequence Read Archive (SRA, <https://www.ncbi.nlm.nih.gov/sra/>) under accession no. SUB8643608, BioProject: PRJNA681969.

5' and 3' RACE

The full-length sequence of *FDNCR* was obtained using a 5'-RACE/3'-RACE kit (Thermo Fisher Scientific, MA, USA), according to the manufacturer's instructions. 5'-RACE and 3'-RACE were performed by nested PCR for each reaction. The abridged anchor and abridged universal anchor primers supplied with the kit were used. Specific primers are listed in Tables S12.

miRNA prediction for targeting *FDNCR* and *DCN*

DCN 3' UTR and *FDNCR* sequences were obtained from NCBI (XM_012159321.3) and this study, respectively. Interactions involving miRNA-mRNA and *FDNCR*-miRNA were predicted based on the mature miRNA sequence of sheep using RNAhybrid (<https://bibiserv.cebitec.uni-bielefeld.de/rnahybrid>) and miRanda (<https://www.miranda-ng.org/en/>). Additionally, mature miRNA sequences from different species were obtained from miRBase (<http://www.mirbase.org>).

Vector construction

The full-length *FDNCR* and coding DNA sequence region (GenBank: NM_001009218.1) of *DCN* were cloned into a pcDNA3.1 overexpression vector. *FDNCR* or *DCN* 3' UTR fragments containing potential miR-543-3p MRE motifs were isolated and inserted into pmirGLO. siRNAs (siRNA-*FDNCR* and siRNA-*DCN*) and miR-543-3p mimics and inhibitor, in addition to the corresponding NC, were synthesized by GenePharma (Shanghai, China; Table S13).

Ovarian GC culture treatments and follicle size classification

Hu sheep ovaries were collected from a local abattoir (Taicang, Jiangsu, China; 121°10'E, 31°45'N) during the breeding season (October to January). GCs were isolated from healthy follicles (2–5 mm) and cultured as previously described.⁶³ Briefly, GCs were seeded into different plates (6 wells, 1 × 10⁶ cells/well; 12 wells,

Figure 5. miR-543-3p regulates GC proliferation and apoptosis and mediates *FDNCR* function

(A) GC apoptosis was detected using flow cytometry. (B and C) mRNA (B) and protein (C) expression of apoptosis-related genes in the GCs in each group. (D–F) GC proliferation was detected using EdU (D and E) and CCK8 (F). Scale bars, 50 μ m. (G) Expression of cell cycle-related genes in the GCs in each group. (H and I) Apoptosis (H) and expression of apoptosis-related genes (I) were detected using flow cytometry and qRT-PCR, respectively. Values represent means \pm SEM for three individuals. *p < 0.05.

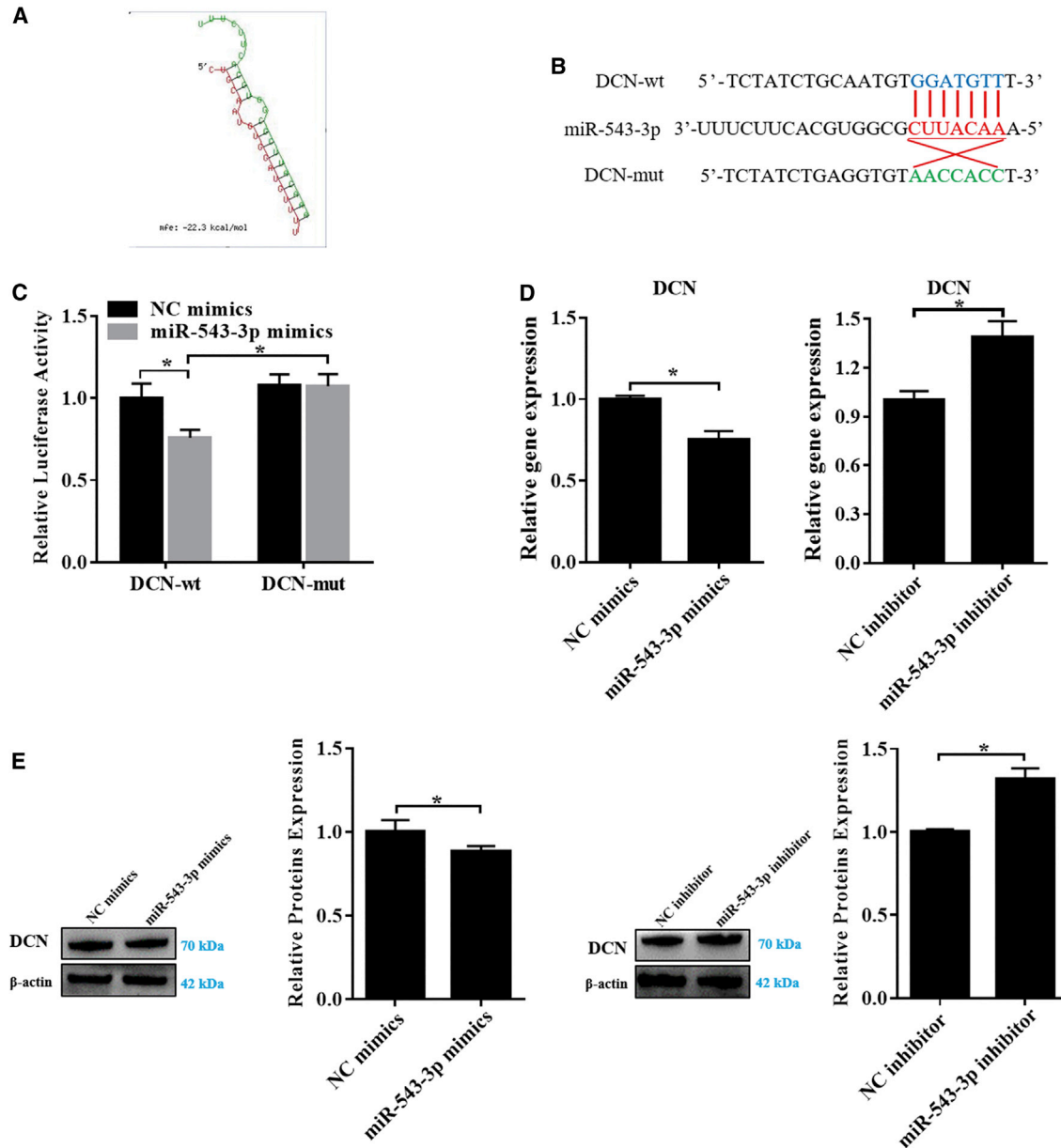
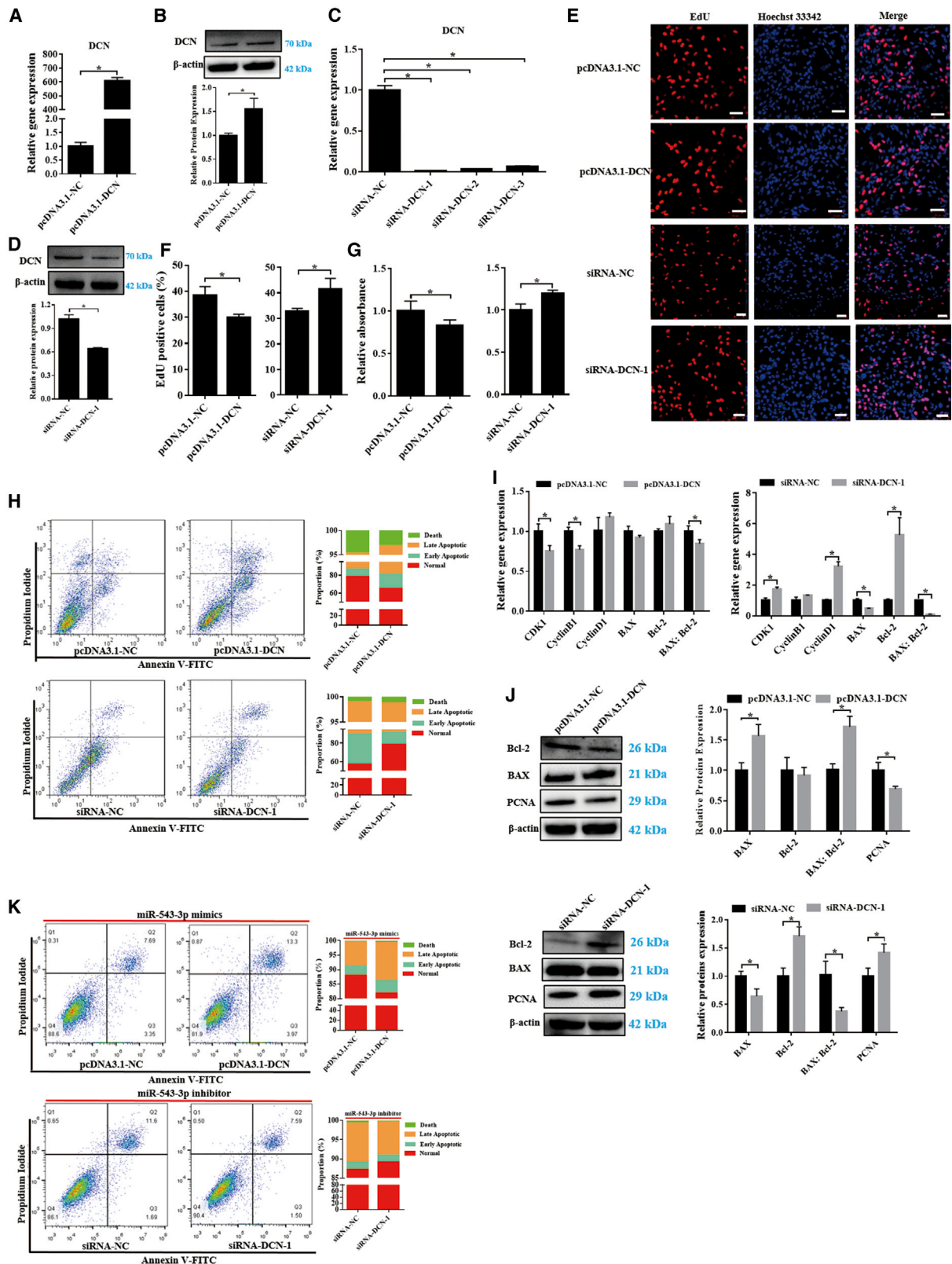


Figure 6. *DCN* is a direct target of miR-543-3p in the GCs of Hu sheep

(A) miRNA-response elements (MREs) within the 3' UTR of sheep *DCN* that enable the binding of miR-543-3p were predicted using RNAhybrid. mfe, minimum free energy. (B) Schematic depicting the interaction of miR-543-3p with wild-type (blue) and mutant *DCN* (green). Red nucleotides indicate the seed sequence of miR-543-3p. (C) The regulatory relationship between miR-543-3p and *DCN* was assessed using a dual-luciferase reporter gene assay. (D and E) Expression of *DCN* mRNA (D) and protein (E) was detected in each group. Values represent means \pm SEM for three individuals. * $p < 0.05$.

5×10^5 cells/well; 24 wells, 1×10^5 cells/well; 96 wells, 1×10^4 cells/well) in culture medium (Dulbecco's modified Eagle's medium/nutrient mixture F-12 [DMEM/F12] supplemented with 10% fetal bovine serum [FBS], 2 mM L-glutamine, 100 IU/mL penicillin, and 100 μ g/mL streptomycin) at 37°C in a humidified atmosphere containing 5% CO₂. After overnight incubation (at 60%~70% conflu-

ence), transfection or co-transfection were performed using Lipofectamine 3000 (Invitrogen, Shanghai, China) for 48 h. 100 nM/mL siRNA-FDNCR, siRNA-*DCN*, and miR-543-3p mimics and inhibitor and 1.25 μ g/mL pcDNA3.1-FDNCR and pcDNA3.1-*DCN* plasmid were used in this study. RNA-seq was performed to identify genes downstream of *DCN* by silencing *DCN* in GCs from Hu sheep. The



(legend on next page)

full datasets have been submitted to NCBI SRA (accession no. SUB8657413, BioProject: PRJNA681969). All visible antral follicles were dissected, measured with a caliper, and classified into three size classes (<3, 3–5, and >5 mm) of approximately 30 ovaries. In total, 18 large follicles (>5 mm), 36 medium follicles (3–5 mm), and 80 small follicles (<3 mm) were collected. Subsequently, three follicles were randomly selected for DCN mRNA level analysis from the large category, while three pooled samples were formed from all collected follicles for the medium and small categories. All reagents used in this study were purchased from Life Technologies (Pleasanton, CA, USA), unless otherwise mentioned.

Cell proliferation analysis

Cell proliferation was analyzed using CCK8 (KeyGen, Nanjing, China) and EdU incorporation assays (KeyGen, Nanjing, China), as described previously.^{64,65} Nuclei were stained with Hoechst 33342.

Cell apoptosis analysis

Cell apoptosis was analyzed by flow cytometry (BD Biosciences, NJ, USA) using an annexin V-fluorescein isothiocyanate/propidium iodide apoptosis detection kit (Vazyme, Nanjing, China). All data were analyzed using FlowJo software.

Immunohistochemistry and immunofluorescence

Immunohistochemistry was performed following our previously described method.⁶⁶ Rabbit anti-DCN and goat anti-rabbit immunoglobulin G (IgG) were the primary and secondary antibodies, respectively. The negative controls were incubated with Tris-buffered saline instead of primary antibodies. All sections were stained with diaminobenzidine (DAB; Boster, Wuhan, China) and examined with a light microscope (Nikon, Tokyo, Japan). All antibodies were purchased from commercial suppliers (Table S14).

Immunofluorescence analysis was performed as described previously.⁶⁷ Rabbit anti-DCN and Coralite 594-conjugated goat anti-rabbit IgG were used as primary and secondary antibodies, respectively. Nuclei were stained with DAPI and examined with an LSM 710 laser scanning confocal microscope (Carl Zeiss, Oberkochen, Germany).

FISH analysis

RNA FISH analysis was performed to assess *FDNCR* localization in GCs using a FISH kit (GenePharma, Shanghai, China) and an *FDNCR* FISH probe mix (Cy3 labeled), following the manufacturer's instructions. 18S was used as a positive control for cytoplasmic fractions. Nuclei were stained with DAPI. Images were captured using an LSM 710 laser scanning confocal microscope.

qRT-PCR analysis

Total RNA extraction and cDNA synthesis were performed as described previously.^{68,69} All qRT-PCR reactions were performed in an ABI 7500 real-time PCR system (Applied Biosystems) using SYBR Green master mix (Roche, Mannheim, Germany) following the manufacturer's instructions. Briefly, the reaction was performed at 95°C for 5 min, followed by 40 cycles of 95°C for 10 s, 60°C for 30 s, and a dissociation step consisting of 95°C for 15 s, 60°C for 15 s, and 95°C for 15 s. miR-16b (for miRNA) and *GAPDH* were used as internal controls. Primer sequences are listed in Tables S15 and S16. The $2^{-\Delta\Delta CT}$ method was used to analyze relative expression levels.

RIP assay

A RIP assay was performed using a RIP assay kit (Sigma-Aldrich, St. Louis, MO, USA) according to the manufacturer's instructions. Briefly, GCs were collected and lysed using RIP lysis buffer. Then, the cell lysates were incubated with magnetic beads conjugated with anti-Ago2 antibody (Abcam, Cambridge, UK). Thereafter, the RNA-protein complex was extracted, and the abundance of *FDNCR* and miR-543-3p in bound fractions was evaluated using qRT-PCR analysis.

Subcellular localization

For nuclear and cytoplasmic RNA separation, 1×10^6 cells were collected and extracted using a Paris kit (Life Technologies, Pleasanton, CA, USA), according to the manufacturer's instructions. *U6* and *GAPDH* were used as positive controls for the nucleus and cytoplasm, respectively.

Western blot analysis

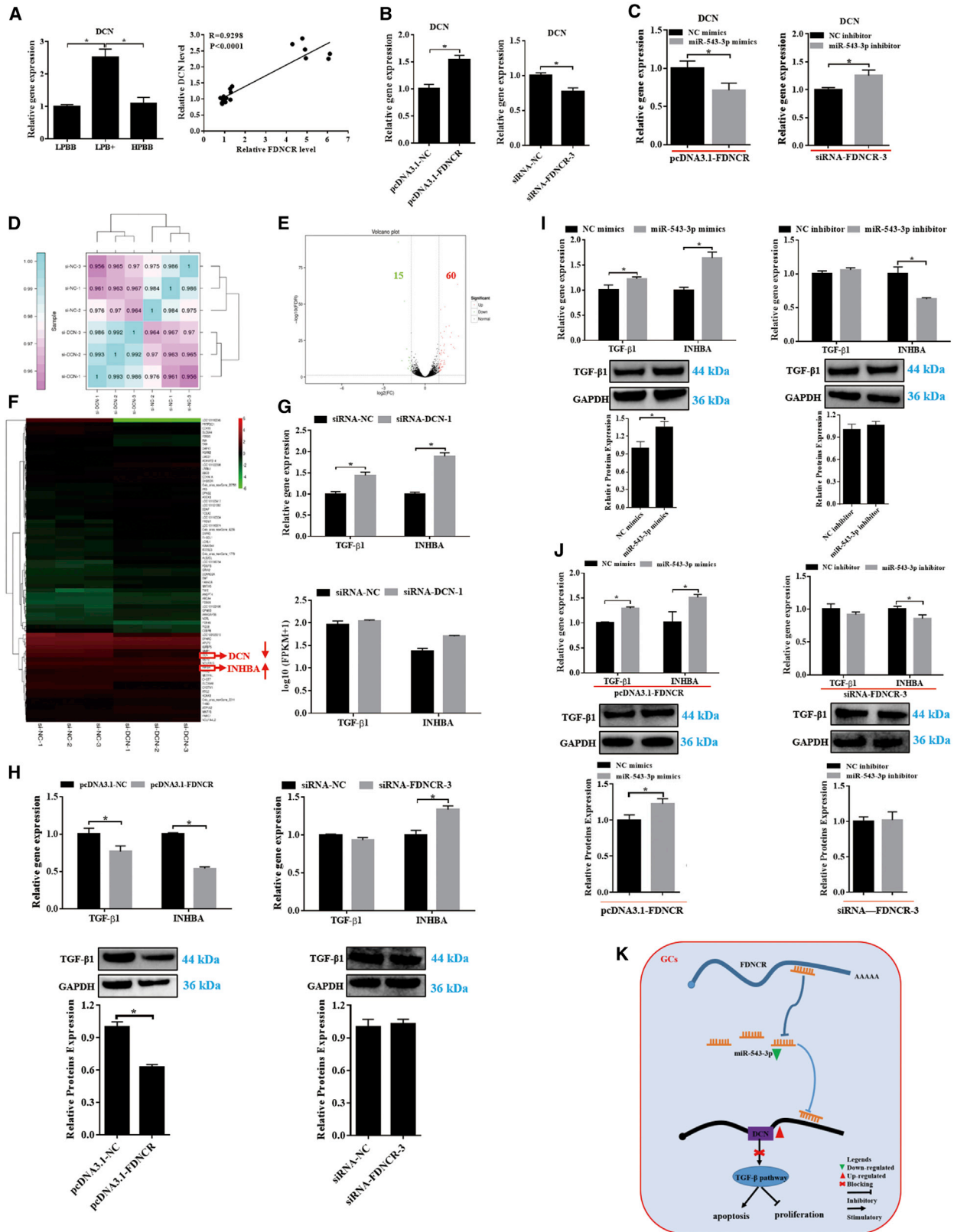
Western blotting was performed according to our previously described methods with slight modification.⁶⁶ Briefly, rabbit anti-DCN, anti-BAX, anti-Bcl-2, anti-PCNA, anti- β -actin, anti-TGF- β 1, and mouse anti-GAPDH were used as primary antibodies, while goat anti-rabbit IgG and goat anti-mouse IgG were used as the secondary antibodies. Immunoreactions were visualized using an enhanced chemiluminescence detection system (Fujifilm, Tokyo, Japan). The protein band intensity was quantified using ImageJ software.

Dual-luciferase reporter assays

After 48 h of transfection, GCs were collected and luciferase activity was determined using the Dual-Luciferase reporter assay system (Vazyme, Nanjing, China), according to the manufacturer's protocol.

Figure 7. miR-543-3p enhances GC proliferation by targeting DCN

(A–D) DCN expression at mRNA and protein levels in the GCs in each group. (E–H) GC proliferation and apoptosis were detected using EdU (E and F), CCK8 (G), and flow cytometry (H). Scale bars, 50 μ m. (I and J) mRNA (I) and protein (J) expression of cell cycle- and/or apoptosis-related genes in the GCs in each group. (K) GC apoptosis in each group was detected using flow cytometry. Values represent means \pm SEM for three individuals. * $p < 0.05$.



(legend on next page)

Statistical analysis

All experiments were performed at least three times. Data are presented as means \pm standard error of the mean based on three independent experiments. All data were normally distributed, and variance was similar between the statistically compared groups. Statistical analyses were performed using GraphPad Prism 6 (GraphPad, San Diego, CA, USA). A Student's t test (two-tailed) or one-way analysis of variance (ANOVA) was performed followed by the Student-Newman-Keuls (SNK) method for multiple comparisons. p values <0.05 were considered statistically significant.

SUPPLEMENTAL INFORMATION

Supplemental information can be found online at <https://doi.org/10.1016/j.omtn.2021.02.030>.

ACKNOWLEDGMENTS

This work was supported by the earmarked funds for the National Natural Science Foundation of China (31872357 and 32002174) and by the Fundamental Research Funds for the Central Universities (KYYJ202001). We sincerely thank Shijia Ying and Rihong Guo from the Jiangsu Academy of Agricultural Sciences for their full support.

AUTHOR CONTRIBUTIONS

F.W. and X.Y. designed the study, and X.Y., X.G., and Y.B. performed the experiments and drafted the manuscript. J.Y., X.L., and Z.W. assisted in conducting the experiments and analyzed the data. X.Y., X.G., and Z. W. collected tissue samples. M.A.E.-S., G.Z., Y.Z., F.W., and W.L. assisted in revision of the manuscript.

DECLARATION OF INTERESTS

The authors declare no competing interests.

REFERENCES

- Yue, G.H. (1996). Reproductive characteristics of Chinese Hu sheep. *Anim. Reprod. Sci.* *44*, 223–230.
- McGee, E.A., and Hsueh, A.J.W. (2000). Initial and cyclic recruitment of ovarian follicles. *Endocr. Rev.* *21*, 200–214.
- Chu, M.X., Liu, Z.H., Jiao, C.L., He, Y.Q., Fang, L., Ye, S.C., Chen, G.H., and Wang, J.Y. (2007). Mutations in BMPR-1B and BMP-15 genes are associated with litter size in Small Tailed Han sheep (*Ovis aries*). *J. Anim. Sci.* *85*, 598–603.
- Fabre, S., Pierre, A., Mulsant, P., Bodin, L., Di Pasquale, E., Persani, L., Monget, P., and Monniaux, D. (2006). Regulation of ovulation rate in mammals: contribution of sheep genetic models. *Reprod. Biol. Endocrinol.* *4*, 20.
- Gootwine, E., Reicher, S., and Rozov, A. (2008). Prolificacy and lamb survival at birth in Awassi and Assaf sheep carrying the FecB (Booroola) mutation. *Anim. Reprod. Sci.* *108*, 402–411.
- Salmena, L., Poliseno, L., Tay, Y., Kats, L., and Pandolfi, P.P. (2011). A ceRNA hypothesis: the Rosetta Stone of a hidden RNA language? *Cell* *146*, 353–358.
- Li, Q.Y., Yang, K., Liu, F.G., Sun, X.G., Chen, L., Xiu, H., and Liu, X.S. (2020). Long noncoding RNA CASC2c inhibited cell proliferation in hepatocellular carcinoma by inactivated ERK1/2 and Wnt/ β -catenin signaling pathway. *Clin. Transl. Oncol.* *22*, 302–310.
- Zhou, X.B., Lai, L.F., Xie, G.B., Ding, C., Xu, X., and Wang, Y. (2020). lncRNA GAS5 sponges miRNA-221 to promote neurons apoptosis by up-regulated PUMA under hypoxia condition. *Neurol. Res.* *42*, 8–16.
- Kang, X., Zhao, Y., Van Arsdell, G., Nelson, S.F., and Touma, M. (2020). Ppp1r1b-lncRNA inhibits PRC2 at myogenic regulatory genes to promote cardiac and skeletal muscle development in mouse and human. *RNA* *26*, 481–491.
- Wu, T., Wang, S., Wang, L., Zhang, W., Chen, W., Lv, X., Li, Y., Hussain, Z., and Sun, W. (2020). Long noncoding RNA (lncRNA) CTTN-IT1 elevates skeletal muscle satellite cell proliferation and differentiation by acting as ceRNA for YAP1 through absorbing miR-29a in Hu sheep. *Front. Genet.* *11*, 843.
- Dasgupta, P., Kulkarni, P., Majid, S., Hashimoto, Y., Shiina, M., Shahryari, V., Bhat, N.S., Tabatabai, L., Yamamura, S., Saini, S., et al. (2020). lncRNA CDKN2B-AS1/miR-141/cyclin D network regulates tumor progression and metastasis of renal cell carcinoma. *Cell Death Dis.* *11*, 660.
- Wang, Y., Li, D., Lu, J., Chen, L., Zhang, S., Qi, W., Li, W., and Xu, H. (2020). Long noncoding RNA TTN-AS1 facilitates tumorigenesis and metastasis by maintaining TTN expression in skin cutaneous melanoma. *Cell Death Dis.* *11*, 664.
- Trovero, M.F., Rodríguez-Casuriaga, R., Romeo, C., Santiañaque, F.F., François, M., Folle, G.A., Benavente, R., Sotelo-Silveira, J.R., and Geisinger, A. (2020). Revealing stage-specific expression patterns of long noncoding RNAs along mouse spermatogenesis. *RNA Biol.* *17*, 350–365.
- Rolland, A.D., Evrard, B., Darde, T.A., Le Béguet, C., Le Bras, Y., Bensalah, K., Lavoué, S., Jost, B., Primig, M., Dejucq-Rainsford, N., et al. (2019). RNA profiling of human testicular cells identifies syntenic lncRNAs associated with spermatogenesis. *Hum. Reprod.* *34*, 1278–1290.
- Chen, Y., Wang, J., Fan, Y., Qin, C., Xia, X., Johnson, J., and Kallen, A.N. (2019). Absence of the long noncoding RNA H19 results in aberrant ovarian STAR and progesterone production. *Mol. Cell. Endocrinol.* *490*, 15–20.
- Li, D., Jiang, W., Jiang, Y., Wang, S., Fang, J., Zhu, L., Zhu, Y., Yan, G., Sun, H., Chen, L., and Zhang, N. (2019). Preliminary functional inquiry of lncRNA ENST00000433673 in embryo implantation using bioinformatics analysis. *Syst Biol Reprod Med* *65*, 164–173.
- Wu, M., Zhang, S., Chen, X., Xu, H., and Li, X. (2019). Expression and function of lncRNA MALAT-1 in the embryonic development of zebrafish. *Gene* *680*, 65–71.
- Ernst, E.H., Nielsen, J., Ipsen, M.B., Villesen, P., and Lykke-Hartmann, K. (2018). Transcriptome analysis of long non-coding RNAs and genes encoding paraspeckle proteins during human ovarian follicle development. *Front. Cell Dev. Biol.* *6*, 78.
- Huang, X., Pan, J., Wu, B., and Teng, X. (2018). Construction and analysis of a lncRNA (PWRN2)-mediated ceRNA network reveal its potential roles in oocyte nuclear maturation of patients with PCOS. *Reprod. Biol. Endocrinol.* *16*, 73.
- Kong, Y., Yao, G., He, J., Yang, G., Kong, D., and Sun, Y. (2018). lncRNA LNC-GULP1-2:1 is involved in human granulosa cell proliferation by regulating COL3A1 gene. *Fertil. Steril.* *110* (4, Suppl), E320.
- Zhao, J., Xu, J., Wang, W., Zhao, H., Liu, H., Liu, X., Liu, J., Sun, Y., Dunaif, A., Du, Y., and Chen, Z.J. (2018). Long non-coding RNA LINC-01572:28 inhibits granulosa cell growth via a decrease in p27 (Kip1) degradation in patients with polycystic ovary syndrome. *EBioMedicine* *36*, 526–538.
- Liu, G., Liu, S., Xing, G., and Wang, F. (2020). lncRNA PVT1/microRNA-17-5p/PTEN axis regulates secretion of E2 and P4, proliferation, and apoptosis of ovarian granulosa cells in PCOS. *Mol. Ther. Nucleic Acids* *20*, 205–216.

Figure 8. *FDNCR* regulates *DCN* and TGF- β signaling pathways by affecting the levels of miR-543-3p in the GCs of Hu sheep

(A) *DCN* expression in the ovaries in each group. Pearson's correlation between *FDNCR* and miR-543-3p. (B and C) Expression of *DCN* in the GCs in each group. (D) Correlation coefficient between siRNA-NC and siRNA-*DCN*. (E) Volcano plot showing the DE genes between the siRNA-NC and siRNA-*DCN* groups. Red indicates up-regulated, green indicates downregulated genes. (F) Hierarchical clustering showing DE genes between the siRNA-NC group and siRNA-*DCN* group. (G) Validation of TGF- β 1 and *INHBA* mRNA expression in different groups. (H–J) mRNA or protein expression of TGF- β 1 and *INHBA* in the GCs in each group. (K) Proposed model of *FDNCR* regulation of GCs state in Hu sheep. RNA-seq data are presented as the $\log_{10}(\text{FPKM}+1)$ of each transcript. Values represent means \pm SEM for three individuals. *p <0.05 .

23. Jiang, B., Xue, M., Xu, D., Song, J., and Zhu, S. (2020). Down-regulated lncRNA HOTAIR alleviates polycystic ovaries syndrome in rats by reducing expression of insulin-like growth factor 1 via microRNA-130a. *J. Cell. Mol. Med.* *24*, 451–464.
24. Taylor, D.H., Chu, E.T.J., Spektor, R., and Soloway, P.D. (2015). Long non-coding RNA regulation of reproduction and development. *Mol. Reprod. Dev.* *82*, 932–956.
25. Miao, X., Luo, Q., Zhao, H., and Qin, X. (2016). Ovarian transcriptomic study reveals the differential regulation of miRNAs and lncRNAs related to fecundity in different sheep. *Sci. Rep.* *6*, 35299.
26. Feng, X., Li, F., Wang, F., Zhang, G., Pang, J., Ren, C., Zhang, T., Yang, H., Wang, Z., and Zhang, Y. (2018). Genome-wide differential expression profiling of mRNAs and lncRNAs associated with prolificacy in Hu sheep. *Biosci. Rep.* *38*, BSR20171350.
27. Miao, X., Luo, Q., Zhao, H., and Qin, X. (2016). Co-expression analysis and identification of fecundity-related long non-coding RNAs in sheep ovaries. *Sci. Rep.* *6*, 39398.
28. Miao, X., Luo, Q., Zhao, H., and Qin, X. (2017). An integrated analysis of miRNAs and methylated genes encoding mRNAs and lncRNAs in sheep breeds with different fecundity. *Front. Physiol.* *8*, 1049.
29. Zheng, J., Wang, Z., Yang, H., Yao, X., Yang, P., Ren, C., Wang, F., and Zhang, Y. (2019). Pituitary transcriptomic study reveals the differential regulation of lncRNAs and mRNAs related to prolificacy in different FecB genotyping sheep. *Genes (Basel)* *10*, 157.
30. Gao, X., Yao, X., Wang, Z., Li, X., Li, X., An, S., Wei, Z.Y., Zhang, G.M., and Wang, F. (2020). Long non-coding RNA366.2 controls endometrial epithelial cell proliferation and migration by upregulating WNT6 as a ceRNA of miR-1576 in sheep uterus. *Biochim. Biophys. Acta Gene Regul. Mech* *1863*, 194606.
31. La, Y., Tang, J., He, X., Di, R., Wang, X., Liu, Q., Zhang, L., Zhang, X., Zhang, J., Hu, W., and Chu, M. (2019). Identification and characterization of mRNAs and lncRNAs in the uterus of polytocous and monotocous Small Tail Han sheep (*Ovis aries*). *PeerJ* *7*, e6938.
32. Ling, Y., Xu, L., Zhu, L., Sui, M., Zheng, Q., Li, W., Liu, Y., Fang, F., and Zhang, X. (2017). Identification and analysis of differentially expressed long non-coding RNAs between multiparous and uniparous goat (*Capra hircus*) ovaries. *PLoS ONE* *12*, e0183163.
33. Matsuda, F., Inoue, N., Manabe, N., and Ohkura, S. (2012). Follicular growth and atresia in mammalian ovaries: regulation by survival and death of granulosa cells. *J. Reprod. Dev.* *58*, 44–50.
34. Lu, C.L., Yang, W., Hu, Z.Y., and Liu, Y.X. (2005). Granulosa cell proliferation differentiation and its role in follicular development. *Chin. Sci. Bull.* *50*, 2665–2671.
35. Zhao, F., Zhao, W., Ren, S., Fu, Y., Fang, X., Wang, X., and Li, B. (2014). Roles of SIRT1 in granulosa cell apoptosis during the process of follicular atresia in porcine ovary. *Anim. Reprod. Sci.* *151*, 34–41.
36. Asselin, E., Xiao, C.W., Wang, Y.F., and Tsang, B.K. (2000). Mammalian follicular development and atresia: role of apoptosis. *Biol. Signals Recept.* *9*, 87–95.
37. Du, X., Liu, L., Li, Q., Zhang, L., Pan, Z., and Li, Q. (2020). NORFA, long intergenic noncoding RNA, maintains sow fertility by inhibiting granulosa cell death. *Commun. Biol.* *3*, 131.
38. Hausser, H., Gröning, A., Hasilik, A., Schönherr, E., and Kresse, H. (1994). Selective inactivity of TGF- β /decorin complexes. *FEBS Lett.* *353*, 243–245.
39. Comalada, M., Cardó, M., Xaus, J., Villedor, A.F., Lloberas, J., Ventura, F., and Celada, A. (2003). Decorin reverses the repressive effect of autocrine-produced TGF- β on mouse macrophage activation. *J. Immunol.* *170*, 4450–4456.
40. Baghy, K., Iozzo, R.V., and Kovacszy, I. (2012). Decorin-TGF β axis in hepatic fibrosis and cirrhosis. *J. Histochem. Cytochem.* *60*, 262–268.
41. Perks, C.M., Newcomb, P.V., Grohmann, M., Wright, R.J., Mason, H.D., and Holly, J.M.P. (2003). Prolactin acts as a potent survival factor against C2-ceramide-induced apoptosis in human granulosa cells. *Hum. Reprod.* *18*, 2672–2677.
42. Diamanti-Kandaraki, E., Argyrakopoulou, G., Economou, F., Kandaraki, E., and Koutsilieris, M. (2008). Defects in insulin signaling pathways in ovarian steroidogenesis and other tissues in polycystic ovary syndrome (PCOS). *J. Steroid Biochem. Mol. Biol.* *109*, 242–246.
43. Jahromi, M.S., Tehrani, F.R., Noroozadeh, M., Zarkesh, M., Ghasemi, A., and Zadeh-Vakili, A. (2016). Elevated expression of steroidogenesis pathway genes; CYP17, GATA6 and STAR in prenatally androgenized rats. *Gene* *593*, 167–171.
44. Li, X., Du, X., Yao, W., Pan, Z., and Li, Q. (2020). TGF- β /SMAD4 signaling pathway activates the HAS2-HA system to regulate granulosa cell state. *J. Cell. Physiol.* *235*, 2260–2272.
45. Bhardwaj, J.K., and Sharma, R.K. (2011). Scanning electron microscopic changes in granulosa cells during follicular atresia in *Caprine* ovary. *Scanning* *33*, 21–24.
46. Zhou, X., Zhang, W., Jin, M., Chen, J., Xu, W., and Kong, X. (2017). lncRNA MIAT functions as a competing endogenous RNA to upregulate DAPK2 by sponging miR-22-3p in diabetic cardiomyopathy. *Cell Death Dis.* *8*, e2929.
47. Li, H., Yang, J., Jiang, R., Wei, X., Song, C., Huang, Y., Lan, X., Lei, C., Ma, Y., Hu, L., and Chen, H. (2018). Long non-coding RNA profiling reveals an abundant MDNCR that promotes differentiation of myoblasts by sponging miR-133a. *Mol. Ther. Nucleic Acids* *12*, 610–625.
48. Qu, C., Dai, C., Guo, Y., Qin, R., and Liu, J. (2020). Long non-coding RNA PVT1-mediated miR-543/SERPIN1 axis plays a key role in the regulatory mechanism of ovarian cancer. *Biosci. Rep.* *40*, BSR20200800.
49. Ma, Z., Gu, G., Pan, W., and Chen, X. (2020). lncRNA PCAT6 accelerates the progression and chemoresistance of cervical cancer through up-regulating ZEB1 by sponging miR-543. *Oncotargets Ther.* *13*, 1159–1170.
50. Yang, F., Ma, J., Tang, Q., Zhang, W., Fu, Q., Sun, J., Wang, H., and Song, B. (2018). MicroRNA-543 promotes the proliferation and invasion of clear cell renal cell carcinoma cells by targeting Krüppel-like factor 6. *Biomed. Pharmacother.* *97*, 616–623.
51. Chen, Z.Y., Du, Y., Wang, L., Liu, X.H., Guo, J., and Weng, X.D. (2018). miR-543 promotes cell proliferation and metastasis of renal cell carcinoma by targeting Dickkopf 1 through the Wnt/ β -catenin signaling pathway. *J. Cancer* *9*, 3660–3668.
52. Du, Y., Liu, X.H., Zhu, H.C., Wang, L., Ning, J.Z., and Xiao, C.C. (2017). miR-543 promotes proliferation and epithelial-mesenchymal transition in prostate cancer via targeting RKIP. *Cell. Physiol. Biochem.* *41*, 1135–1146.
53. Peng, J.Y., Gao, K.X., Xin, H.Y., Han, P., Zhu, G.Q., and Cao, B.Y. (2016). Molecular cloning, expression analysis, and function of decorin in goat ovarian granulosa cells. *Domest. Anim. Endocrinol.* *57*, 108–116.
54. Salgado, R.M., Favaro, R.R., and Zorn, T.M.T. (2011). Modulation of small leucine-rich proteoglycans (SLRPs) expression in the mouse uterus by estradiol and progesterone. *Reprod. Biol. Endocrinol.* *9*, 22.
55. Adam, M., Saller, S., Ströbl, S., Hennebold, J.D., Dissen, G.A., Ojeda, S.R., Stouffer, R.L., Berg, D., Berg, U., and Mayerhofer, A. (2012). Decorin is a part of the ovarian extracellular matrix in primates and may act as a signaling molecule. *Hum. Reprod.* *27*, 3249–3258.
56. Wu, W.X., Zhang, Q., Unno, N., Derks, J.B., and Nathanielsz, P.W. (2000). Characterization of decorin mRNA in pregnant intrauterine tissues of the ewe and regulation by steroids. *Am. J. Physiol. Cell Physiol.* *278*, C199–C206.
57. Yamaguchi, Y., and Ruoslahti, E. (1988). Expression of human proteoglycan in Chinese hamster ovary cells inhibits cell proliferation. *Nature* *336*, 244–246.
58. Hua, X., Liu, Z., Zhou, M., Tian, Y., Zhao, P.P., Pan, W.H., Li, C.X., Huang, X.X., Liao, Z.X., Xian, Q., et al. (2019). LSAMP-AS1 binds to microRNA-183-5p to suppress the progression of prostate cancer by up-regulating the tumor suppressor DCN. *EBioMedicine* *50*, 178–190.
59. Yao, G., Yin, M., Lian, J., Tian, H., Liu, L., Li, X., and Sun, F. (2010). MicroRNA-224 is involved in transforming growth factor- β -mediated mouse granulosa cell proliferation and granulosa cell function by targeting Smad4. *Mol. Endocrinol.* *24*, 540–551.
60. Yang, L., Du, X., Liu, L., Cao, Q., Pan, Z., and Li, Q. (2019). miR-1306 mediates the feedback regulation of the TGF- β /SMAD signaling pathway in granulosa cells. *Cells* *8*, 298.
61. Chu, M., Jia, L., Zhang, Y., Jin, M., Chen, H., Fang, L., Di, R., Cao, G., Feng, T., Tang, Q., et al. (2011). Polymorphisms of coding region of BMPR-IB gene and their relationship with litter size in sheep. *Mol. Biol. Rep.* *38*, 4071–4076.
62. Saito, R., Smoot, M.E., Ono, K., Ruschinski, J., Wang, P.L., Lotia, S., Pico, A.R., Bader, G.D., and Ideker, T. (2012). A travel guide to Cytoscape plugins. *Nat. Methods* *9*, 1069–1076.

63. Zhang, G.M., Deng, M.T., Zhang, Y.L., Fan, Y.X., Wan, Y.J., Nie, H.T., Wang, Z.Y., Wang, F., and Lei, Z.H. (2016). Effect of PGC-1 α overexpression or silencing on mitochondrial apoptosis of goat luteinized granulosa cells. *J. Bioenerg. Biomembr.* 48, 493–507.
64. Li, H., Yang, J., Wei, X., Song, C., Dong, D., Huang, Y., Lan, X., Plath, M., Lei, C., Ma, Y., et al. (2018). circFUT10 reduces proliferation and facilitates differentiation of myoblasts by sponging miR-133a. *J. Cell. Physiol.* 233, 4643–4651.
65. Yao, X., Wang, Z., El-Samahy, M.A., Ren, C., Liu, Z., Wang, F., and You, P. (2020). Roles of vitamin D and its receptor in the proliferation and apoptosis of luteinised granulosa cells in the goat. *Reprod. Fertil. Dev.* 32, 335–348.
66. Yao, X., Yang, H., Zhang, Y., Ren, C., Nie, H., Fan, Y., Zhou, W., Wang, S., Feng, X., and Wang, F. (2017). Characterization of GALNTL5 gene sequence and expression in ovine testes and sperm. *Theriogenology* 95, 54–61.
67. Yao, X., Ei-Samahy, M.A., Fan, L., Zheng, L., Jin, Y., Pang, J., Zhang, G., Liu, Z., and Wang, F. (2018). In vitro influence of selenium on the proliferation of and steroidogenesis in goat luteinized granulosa cells. *Theriogenology* 114, 70–80.
68. Yao, X., Wang, Z., Gao, X., Li, X., Yang, H., Ei-Samahy, M.A., Bao, Y., Xiao, S., Meng, F., and Wang, F. (2020). Unconservative_15_2570409 suppresses progesterone receptor expression in the granulosa cells of Hu sheep. *Theriogenology* 157, 303–313.
69. Yao, X., Zhang, G., Guo, Y., Ei-Samahy, M., Wang, S., Wan, Y., Han, L., Liu, Z., Wang, F., and Zhang, Y. (2017). Vitamin D receptor expression and potential role of vitamin D on cell proliferation and steroidogenesis in goat ovarian granulosa cells. *Theriogenology* 102, 162–173.